

# Lattice hyper-solitons in photorefractive materials

José Ramón Salgueiro, Humberto Michinel and María I. Rodas-Verde  
Área de Óptica, Faculdade de Ciencias de Ourense,  
Universidade de Vigo, As Lagoas s/n, Ourense ES-32004, Spain

We show a novel kind of nonlinear waves in two-dimensional photonic lattices. These waves take the form of light clusters that may fill an arbitrary number of lattice sites. We have demonstrated by numerical simulations that stable propagation can be achieved under adequate conditions and we have described the unstable patterns developed otherwise. Our results show that these new kind of nonlinear waves can be easily found in current experiments.

PACS numbers:

Optical lattices are artificial crystals of light[1] that can be obtained by shining an adequate optical material (usually photorefractive) with a number of mutually coherent laser beams. The interference pattern created by those beams, induces a spatially periodic modulation of the refractive index in the material. This effect can be used to trap a probe laser beam, usually much weaker and of different frequency than those beams used to generate the lattice.

The study of nonlinear waves in periodic potentials has become an active field of research in recent years due to its applications in control and manipulation of light properties. In this kind of systems, the appropriate combination of the probe beam power and the lattice depth and period yields to stable and localized light propagation for the probe laser. This beam, under adequate conditions, can generate a *lattice soliton*[2], linked to a site of the periodic potential, that propagates undistorted.

The generation of lattice solitons has been demonstrated experimentally in both one-dimensional [3, 4] and two-dimensional[5, 6] potentials. Novel kinds of nonlinear waves like soliton dipoles and quadrupoles[7, 8] as well as discrete vortices have been also demonstrated[9, 10]. Most of this results have been generalized for the case of several probe beams that are mutually incoherent, yielding to the so-called *discrete vector solitons*[11].

In this Letter, we will show that all these previous distributions belong to a more general and novel kind of nonlinear waves that exists in two-dimensional periodic lattices. These waves are clusters of parallel laser beams that are linked to the sites of the lattice. The adequate choice of beam powers and lattice parameters yields to the formation of arrays of lattice solitons that propagate without shape distortion for arbitrarily long distances. The extension of this light distributions can be arbitrary large, filling an unlimited number of lattice sites, so they may be regarded as hyper-solitons.

We will calculate the explicit form of these distributions and demonstrate that stable propagation is achieved for a wide range of configurations. We will also test the stability of these structures when they are generated using arrays of Gaussian beams[12, 13] with adequate powers, widths and relative phases, calling in that way for the experimental demonstration.

We will study the paraxial propagation along  $z$  of a

laser beam with envelope  $\Psi(x, y, z)$ , through a photorefractive material with a periodic modulation of the refractive index in the transversal plane  $(x, y)$ . This process can be described by the following wave equation [11],

$$i \frac{\partial \Psi}{\partial z} + \Delta_{\perp} \Psi - \frac{\Psi}{1 + V(x, y) + |\Psi|^2} = 0, \quad (1)$$

where  $\Delta_{\perp}$  is the transverse Laplacian operator, the spatial variables  $x$  and  $y$  are expressed in units of the wavelength ( $\lambda$ ) and  $z$  is measured in units of  $4\pi\lambda$ . The function  $V(x, y) = A \cos^2(\pi x/T) \cos^2(\pi y/T)$  defines the periodic optically-induced lattice, where  $A$  and  $T$  are respectively its amplitude and period. Both parameters can be easily controlled by acting on the laser beams that generate the grid.

We look for stationary solutions of the form  $\Psi(x, y, z) = u(x, y) \exp(i\beta z)$ , where  $\beta$  is the propagation constant. These solutions can be numerically calculated and constitute families of solitons described by the parameter  $\beta$ . In Fig. 1 we show some examples of stationary states for the particular values of the parameters,  $A = 1$ ,  $T = 10$ . In order to have localized solutions with  $u(x, y \rightarrow \pm\infty) = 0$ , due to the particular form of the potential term in Eq. (1), it is required that  $\beta < 0$ .

Each family of solitons is topologically defined by the number of lobes and phase configuration. In Fig. 2, we show plots of the power  $P = \int_{-\infty}^{\infty} |u|^2 dx dy$  versus the propagation constant for several families of solitons, corresponding to different cases illustrated in Fig. 1.

In the linear limit, the periodicity of the medium requires Bloch-type periodic solutions (see Fig. 1-A), which extend over the whole lattice. If the nonlinear effect is significant, localized solutions appear, taking the form of multi-hump solitons whose lobes are located at the maxima of the lattice. It can be appreciated that families of solitons with a higher number of lobes present a higher power. For a particular family, the shape and amplitude of the lobes depend on the value of the propagation constant, so that  $P$  basically increases with  $\beta$ .

In Fig. 1-B,C it is shown that as power raises, two close lobes of the same sign undergo fusion into a single lobe state (Fig. 1-D) centered at a lattice nodal line, which may reach unlimited high values. This is due to the nonlinear effect which shades the lattice for high powers.

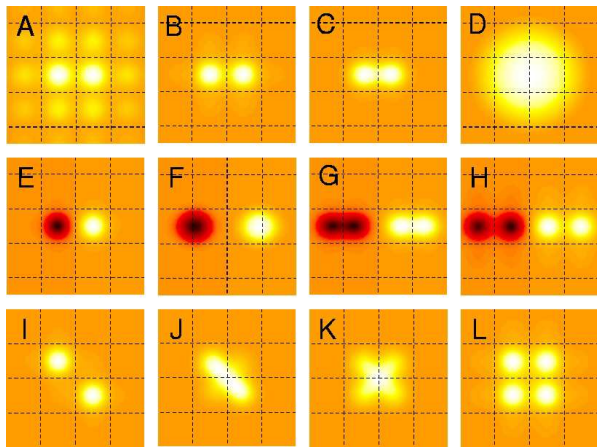


FIG. 1: Plots of the amplitude of different multi-hump solitons, illustrating the dependence of their shapes with power (or  $\beta$ ). Dashed lines indicate the nodes of the lattice. Labels correspond to points in Fig. 2.

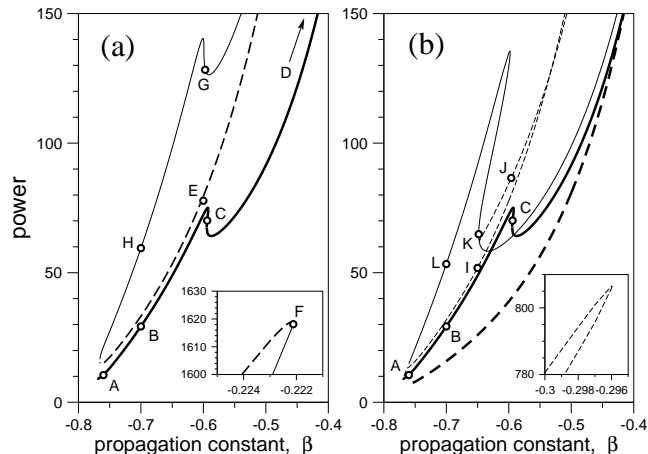


FIG. 2: Power curves for different families of multi-hump solitons. (a) Solitons with two side by side light spots (continuous thick line: two same-phase lobes; dashed line: same but inverted phase; continuous thin line: two double-hump spots with inverted phase). (b) Solitons with lobes of the same relative phase and disposed in different configurations (thick dashed: one lobe; thick continuous: two side by side lobes; thin dashed: two diagonally disposed lobes; thin continuous: four lobes disposed in a two by two array). Letters label points corresponding to the examples in Fig. 1. Point D, out of the frame, has coordinates  $(-0.02, 1.45 \times 10^5)$ .

Modes with two inverted-phase lobes (Fig. 1-E) exhibit a different behavior with power. Neighbor lobes prevent each other from growing up, increasing power arbitrarily with  $\beta$ . Instead, the lobes drift away from each other, also increasing their width, up to the point where they are located on lattice nodal lines (Fig. 1-F). There, the power curve reaches an end point where branches corresponding to other families join (see Fig. 2-(a)). This is the case for the family of solitons composed by four lobes disposed in a two double-lobe configuration (Fig. 1-H). For this

family, increasing  $\beta$  yields to a fusion of the same-sign doublets (Fig. 1-G) ending with the state in Fig. 1-F.

Fusion and splitting of lobes always correspond to an inversion in the sign of the slope of the  $P$  vs  $\beta$  curve and this inverted-slope section of the curve is more pronounced as many lobes are involved in the fusion (see for instance thick and thin continuous lines in Fig 2-(b), corresponding to two and four lobe family respectively). Analogous fusion or splitting take place for states with diagonally-disposed lobes (see Fig. 1-I). In this case, the fusion takes place towards a fundamental soliton centered at a node in the common corner of both lattice sites (Figs. 1-J,K).

In cases where an odd number of symmetrically disposed lobes does not permit a preferential fusion of two of them, a new scenario appears. For example the family of soliton M (Fig. 3), changes when  $\beta$  is increased, lowering the amplitude of the central lobe up to the point where it disappears. Soliton N, however, does not qualitatively change.

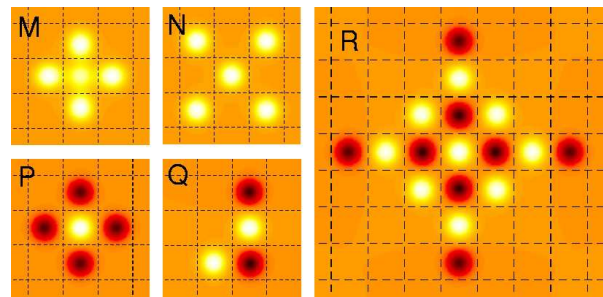


FIG. 3: Examples of higher-order solitons, showing different configurations, including one with a large number of humps (labeled R). For all of them  $\beta = -0.5$ . Dashed lines indicate the zeros of the lattice.

States with a higher number of lobes present more complicated dependences of the shape with power, and they can be basically accounted in terms of the same effects described above. An example is the two-by-two lobe soliton (L) whose lobes also merge together at the negative slope region of the curve. On the other hand, branches corresponding to different solitons may join together at point (K) where the two and four lobe solitons fuse into a fundamental one.

The stability of those hyper-solitons was investigated by means of numerical simulations using a standard Beam Propagation Method. The evolution of the maximum amplitude for some states is plotted in Fig. 4. The first conclusion is that those states whose lobes alternate sign are completely stable (for instance, all those corresponding to the dashed line in fig. 2(a)). Lines E, P, Q and R in Fig. 4-(a), correspondent to the same label solitons in Figs. 1 and 3, confirm the stability of those states. The numerical simulations were also carried out using arrays of Gaussian beams instead of the exact eigenstates and they resulted stable as well. This robustness would

eventually allow to reproduce the results experimentally and make this beams suitable to be used for optical control operations.

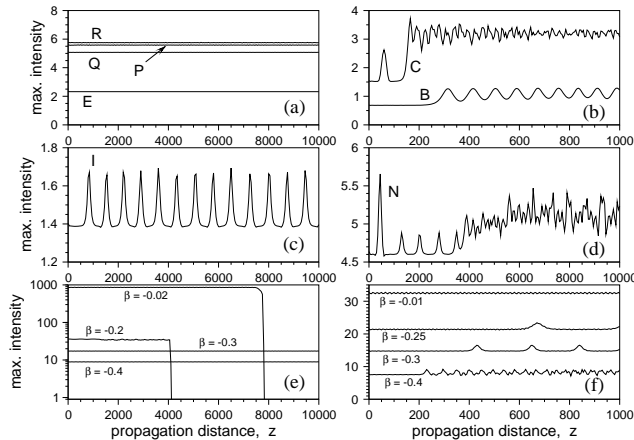


FIG. 4: Maximum amplitude versus propagation constant for a number of states. Line labels correspond to the solitons in Figs. 1 and 3.

Contrariwise, solitons with lobes of the same sign or different sign pattern develop a number of instability scenarios which can be summarized as follows. For low power, the beam lobes are centered at lattice sites and they maintain their position developing power oscillations due to the coupling taking place from one to each other (see line B in Fig. 4-(b)); solitons H, L and M present a similar behavior). For states corresponding to the negative slope region of the power curve, close lobes merge together and oscillate laterally with an amplitude of the order of the lattice pitch. This transversal oscillations also affect the amplitude (line C in Fig. 4-(b)); similar behavior is found for soliton G). Similar oscillations are also found for solitons in the region of the power curve where the slope turns again positive, for moderate power. For

high power, however, the lobes are found to fly off from each other after some propagation distance.

A different scenario is that of states with lobes disposed diagonally. Alternating sign ones remain stable. For those with same sign lobes, however, the instability pattern is different according to the branch of the power curve. Those belonging to one of the branches (solitons I and N for instance), develop a periodic phase (sign) inversion between alternate lobes (see line I in Fig. 4-(c)). Nevertheless, solitons of higher order develop for longer propagation distance more complicated coupling patterns (see line N in Fig. 4-(d)). On the other hand, states belonging to the other branch (like soliton J) develop a fusion of lobes followed by transversal oscillations, similarly to the case of negative slope.

Concerning the fundamental soliton (one lobe) it is stable for low powers when centered at a lattice maximum (see simulations for different powers in Fig. 4-(e)). For higher powers, however, it wanders around, since the lattice is not enough to clamp it to the site, flying away at the end. The propagation distance at which the lobe starts to move increases as power increases and the soliton becomes virtually stable as power tends to infinite. A similar behavior is found when the state is centered on a nodal line (soliton D for instance) or nodal point, but in this case it is unstable for low powers, developing lateral oscillations between two nodal positions (see Fig. 4-(f), simulations for different power D-type solitons).

In conclusion, we have introduced and analyzed novel types of stable discrete solitons in two-dimensional photonic lattices. Our simulations reveal that the experimental demonstration of our results is accessible with standard techniques.

The authors acknowledge support from the Ministerio de Educación y Ciencia of Spain (projects FIS2004-02466, FIS2004-20188-E and Ramón y Cajal contract granted to J. R. Salgueiro) and from Xunta de Galicia (project PGIDIT04TIC383001PR).

- 
- [1] D.N. Christodoulides, F. Lederer, and Y. Silberberg, *Nature* **424**, 817 (2003).
  - [2] D.N. Christodoulides and R.I. Joseph, *Opt. Lett.* **13**, 794 (1988)
  - [3] J.W. Fleischer, T. Carmon, M. Segev, N. K. Efremidis, and D. N. Christodoulides, *Phys. Rev. Lett.* **90**, 023902 (2003).
  - [4] D. Neshev, E.A. Ostrovskaya, Yu. S. Kivshar, and W. Krolikowski, *Opt. Lett.* **28**, 710 (2003).
  - [5] J.W. Fleischer, M. Segev, N. K. Efremidis, and D. N. Christodoulides, *Nature* **422**, 147 (2003).
  - [6] H. Martin, E.D. Eugenieva, Z. Chen, and D.N. Christodoulides, *Phys. Rev. Lett.* **92**, 123902 (2004).
  - [7] J. Yang, I. Makasyuk, A. Bezryadina, and Z. Chen, *Opt. Lett.* **29**, 1662 (2004).
  - [8] J. Yang, I. Makasyuk, A. Bezryadina, and Z. Chen, *Stud. Appl. Math.* **113**, 389 (2004).
  - [9] D.N. Neshev, T.J. Alexander, E.A. Ostrovskaya, Yu.S. Kivshar, H. Martin, and Z. Chen, *Phys. Rev. Lett.* **92**, 123903 (2004).
  - [10] J.W. Fleischer, G. Bartal, O. Cohen, O. Manela, M. Segev, J. Hudock, and D.N. Christodoulides, *Phys. Rev. Lett.* **92**, 123904 (2004).
  - [11] Z. Chen, A. Bezryadina, I. Makasyuk, and Y. Yang, *Opt. Lett.* **29**, 1656 (2004).
  - [12] Y.V. Kartashov, A.A. Egorov, L. Torner, and D.N. Christodoulides, *Opt. Lett.* **29**, 1918 (2004).
  - [13] M. I. Rodas-Verde, H. Michinel, and Yu. S. Kivshar, *Opt. Lett.* (2006) (to be published).